Temperature-insensitive fiber-optic devices using multimode interference effect

Saurabh Mani Tripathi,[1,*] Arun Kumar,[2] Manoj Kumar,[2] and Wojtek J. Bock[1]

[1]*Centre de Recherche en Photonique, Université du Québec en Outaouais, Gatineau (Québec) J8Y 3G5, Canada*

[2]*Department of Physics, Indian Institute of Technology Delhi, New Delhi 110016, India*

**Corresponding author: tripathi.iit@gmail.com*

Received May 7, 2012; revised September 1, 2012; accepted September 13, 2012;
posted September 19, 2012 (Doc. ID 168060); published November 6, 2012

We show theoretically that the fiber-optic devices using single-multi-single mode fiber structures can be made temperature insensitive by properly adjusting the concentration of P_2O_5 in the core region of the multimode fiber used. Taking an example of a parabolic index multimode fiber, we obtain the temperature-insensitive transmission spectrum and fiber-optic lens action for a core composition of 1.57 mol. % P_2O_5 and 13.5 mol. % GeO_2 in the SiO_2 host.

OCIS codes: 060.2340, 050.2770, 010.0280, 060.2370, 120.0280, 130.6010.

Multimode interference (MMI)-based integrated optical devices are well established [1]. In the recent past there has been a renewed interest in realizing various optoelectronic components such as the optical beam shaper [2], tunable band pass/stop filters [3–5], optical switches, and directional couplers [6], fiber lenses [7], and sensors [8–10] based on MMI effects. These devices are very attractive due to their low cost, ease of fabrication, and the freedom they offer in tailoring the output spectrum. However, due to the very nature of the modal interference, they are highly susceptible to external perturbations including temperature variations. A proper packaging and thermal insulation solution is, therefore, a prerequisite for their stable operation, except for their application as temperature sensors.

There are only a few reports of strategies for mitigating the temperature sensitivity of MMIs: (i) Li has suggested a proper device packaging with a suitable ceramic to compensate for the thermal expansion of the optical fiber [11], and (ii) Dong *et al.* have proposed another method based on a precise single-mode fiber-multimode fiber (SMF-MMF) core offset that results in a temperature-insensitive extinction ratio of the transmission spectrum [12–14]. Both of these methods, though offering a quick solution, are extrinsic in nature, giving rise to certain drawbacks including increased device size, complexity associated with the device fabrication, requirement of special postprocessing treatment, and/or necessitation of high-precision splicing. The MMI-based devices, inherently insensitive to temperature variations, have yet not been reported.

In this Letter, we investigate numerically the effect of MMF core dopants on the MMI and show that such fiber-optic devices can be made temperature insensitive by properly adjusting the concentrations of P_2O_5 and GeO_2 in the MMF core. We consider a single-multi-single (SMS) mode fiber-optic structure consisting of a parabolic profiled MMF of length L axially spliced at both its ends to identical step index SMFs. At the first splice, light is launched into the MMF section through the lead-in SMF. Generally, the spot size of the fundamental mode of the MMF is different than that of the SMF. This leads to the excitation of a number of guided modes in the MMF at the input splice. We assume that the MMF is axially aligned with the SMFs at both the ends, which can readily be achieved using commercially available splicing machines. In such a case, only the axially symmetric modes (LP_{0m}) of the MMF will be excited.

The field within the MMF at the first splice can be expressed as $\Psi_M = \Psi_S = \Sigma_m \eta_m \psi_m$, where η_m is the field amplitude, determined by the overlap integral between the fields Ψ_S (of the SMF) and ψ_m (of the mth mode of the MMF). Due to their different propagation constants, the guided modes of the MMF develop a certain phase difference as they propagate along the MMF length. At the lead-out splice the MMF modal fields are then coupled to the fundamental mode of the lead-out SMF. The power in the lead-out fiber can be written as [9,10]

$$P_o = \left| \int_0^\infty \Psi_s^* \Psi_M(L) r \mathrm{d}r \int_0^{2\pi} \mathrm{d}\theta \right|^2 = \left| \sum\nolimits_m \eta_m^2 e^{i(\beta_1 - \beta_m)L} \right|^2. \quad (1)$$

Here, β_m is the propagation constant of mth mode. Utilizing the fact that only the first few modes of the MMF carry most of the power coupled from the SMF (~99% carried by first four modes) [9,10], the ψ_m and β_m can be easily obtained by approximating the MMF core with an infinitely extended parabolic index distribution. Under this approximation, β_m and $\psi_m(r)$ are given by [15]

$$\beta_m = k_0 n_0 \left[1 - \frac{2(2m-1)\alpha_m}{k_0^2 n_0^2} \right]^{1/2} \quad (2)$$

and

$$\psi_m(r) = \sqrt{\frac{2}{\pi}} \frac{1}{w_M} L_{m-1}\left(\frac{2r^2}{w_M^2} \right) e^{-r^2/w_M^2}. \quad (3)$$

Here, $m = 1,2,3\ldots$ and $\alpha_m = (k_0 n_0 / a_M)\sqrt{2\Delta_M} = V_M / a_M^2$, with $V_M = k_0 a_M \sqrt{n_0^2 - n_{cl}^2}$. $L_m(r)$ is the Laguerre polynomial of degree m, and w_M is the Gaussian spot size of the fundamental mode given by $w_M = a_M \sqrt{2/V_M}$. In order to check the validity of infinitely extended parabolic medium approximation, we also calculated the propagation constants of the LP_{01}–LP_{04} modes of the MMF numerically using the multilayer method; the results are

found to match within 0.0005% with that obtained using Eq. (2).

Using the Gaussian approximation for the modal field of the SMF [16], the field amplitude η_m is obtained as

$$\eta_m = \frac{\int_0^\infty \Psi_s \psi_m^* r\mathrm{d}r}{\int_0^\infty |\psi_m|^2 r\mathrm{d}r} = \frac{2\mu}{1+\mu^2}\left(\frac{1-\mu^2}{1+\mu^2}\right)^m \tag{4}$$

with $\mu = w_S/w_M$; w_S is the Gaussian spot size of the SMF.

Finally, the dielectric constant of the MMF core region (ϵ_t) (GeO_2 and P_2O_5 doped SiO_2) is obtained using the Maxwell–Garnet effective medium approximation (EMA) [17–19],

$$\sum_m \frac{\epsilon_m - \epsilon_t}{\epsilon_m + 2\epsilon_t} v_m = 0, \tag{5}$$

which gives better agreement with the experimental values (within 1.9%) as compared to the Lorentz–Lorentz equation [19]. In the above equation, ϵ_m ($= n_m^2$) and v_m are, respectively, the dielectric constant and the volume fraction of the mth component. Using Eq. (5), we first obtained the dielectric constants of *pure* P_2O_5 and GeO_2 using the experimentally reported dielectric constants of 9.1 mol. % "P_2O_5 doped SiO_2" [20] and 13.5 mol. % "GeO_2 doped SiO_2" [21] and that of the fuzed SiO_2 using the Sellmeier relation [22]. Having obtained the dielectric constants of P_2O_5 and GeO_2, the dielectric constant of the core region is then obtained using Eq. (5). The volume fraction v_m of various components is obtained by using the known values of the exact molar mass (sum of the masses of the individual elements of the molecule) and the densities of the binary components as tabulated in Table 1.

In our calculations, we consider the SMF core region to be made of 3.1 mol. % GeO_2 in SiO_2 host and that of the MMF codoped with q mol. % of P_2O_5 and 13.5 mol. % GeO_2 in SiO_2 host. The cladding regions for both the SMF and MMF are made of fused SiO_2. The core diameters of the SMF and MMF are taken as 8.2 and 62.5 μm, respectively. The temperature dependence of the refractive index of ith region has been obtained by using the relation $n_i = n_{0i} + (dn_{0i}/dT)(T - T_0)$, where n_{0i} represents the refractive indices at room temperature T_0. The thermo-optic coefficient dn/dT for fused SiO_2, 15 mol. % GeO_2 doped SiO_2, and P_2O_5 are known to be 1.06×10^{-5} /°C, 1.24×10^{-5} /°C, and -9.22×10^{-5} /°C, respectively [9,10]. Assuming a linear dependence of the thermo-optic coefficient on the dopant concentration [9,10], its value for different dopants has been obtained. The changes in length and core radius with temperature are taken as $\Delta L = \alpha L \Delta T$ and $\Delta a_M = \alpha a_M \Delta T$, respectively. Here α is the thermal expansion coefficient whose value is taken as $\alpha = 5 \times 10^{-7}$ /°C for fused silica [9,10].

Table 1. Physical Parameters of Binary Glasses

	SiO_2	GeO_2	P_2O_5
Molar mass ($g\,mol^{-1}$)	59.96676	105.91101	283.88905
Density ($g\,cm^{-3}$)	2.648	4.228	2.390

Using Eqs. (2), (3), and (5) in Eq. (1), the transmission spectrum of the SMS structure has been obtained for different concentrations of the P_2O_5 in the MMF core, for $L = 41$ cm. In Fig. 1, we have plotted the transmission spectrum for the MMF core with (a) 0, (b) 1.47, (c) 1.57, and (d) 1.67 mol. % P_2O_5 co-doped with 13.5 mol. % GeO_2 in SiO_2 host. The transmission spectra have been shown intentionally near the *critical* wavelength where the MMI-based devices are most sensitive [9,10]. It can be observed from Fig. 1 that (a) without any P_2O_5 in the core, the SMS structure exhibits extremely high temperature sensitivity ~2.78 nm/°C; (b) as the P_2O_5 concentration is increased, the spectral shift starts decreasing, the typical sensitivity being ~0.167 nm/°C for 1.47 mol. % P_2O_5; (c) the sensitivity is ~0 nm/°C for 1.57 mol. % P_2O_5; and (d) with further increase in the P_2O_5 concentration, the transmission spectrum starts moving in the opposite direction as compared to Figs. 1(a) and 1(b) owing to the negative thermo-optic coefficient of the MMF core at higher P_2O_5 concentrations. It is important to mention here that for the ease of fabrication, typically in all the commercial MMFs, generally the P_2O_5 is codoped in the fiber core to reduce the softening temperature. Therefore, by controlling its fraction in the fiber core, temperature-insensitive devices, based on modal interference, can be realized.

Another major branch of application based on the MMI utilizes self-imaging of the propagating modes in the MMF. To study the effect of the P_2O_5 on the self-imaging we first obtain the field pattern across the MMF ($\Psi_{MMF} = \Sigma_m \eta_m \psi_m e^{i\beta_m z}$). Using Eqs. (2), (3), and (5) the field pattern in $y = 0$ plane, obtained at the critical wavelength $\lambda = 0.93$ μm, has been plotted in Fig. 2(a), where following [7] we have removed the lead-out SMF to show the MMI application as a fiber lens, taking the MMF length as 1.01 cm. Two distinct features observed from this figure are (i) unlike the step-index MMF [1,7], no multiple

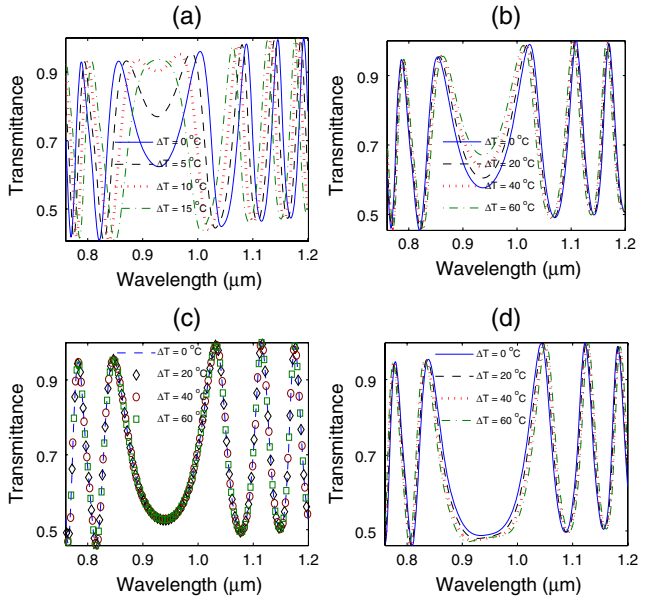

Fig. 1. (Color online) Transmission spectra of the SMS structure using MMF core with (a) 0, (b) 1.47, (c) 1.57, and (d) 1.67 mol. % P_2O_5 codoped with 13.5 mol. % GeO_2 in SiO_2 host.

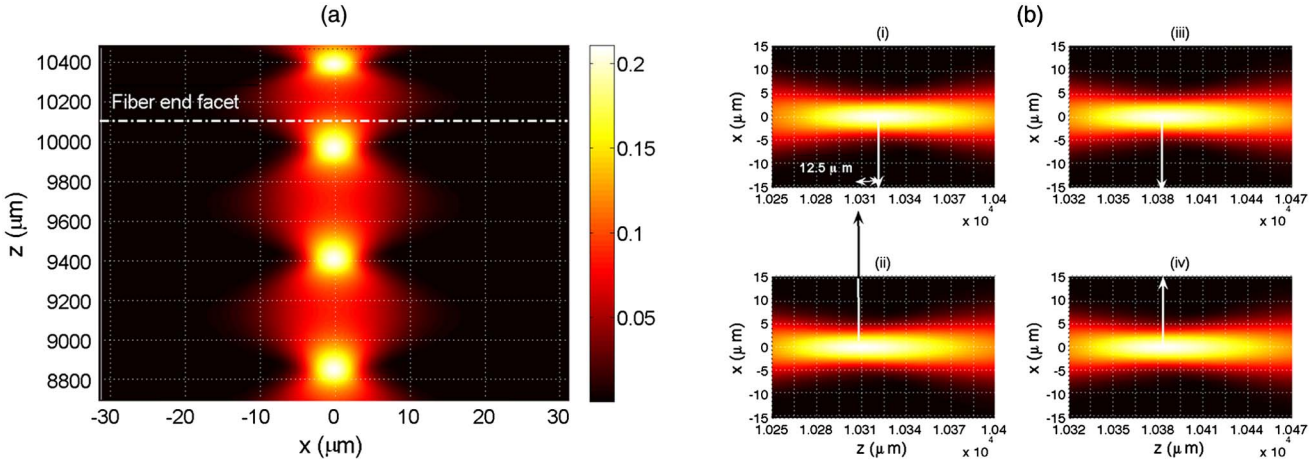

Fig. 2. (Color online) (a) Optical field pattern inside and outside the parabolic core MMF for 1.57 mol. % doping of P_2O_5. (b) Intensity pattern at the exit of MMF showing lens action in air for (i) $\Delta T = 0°C$ and (ii) $\Delta T = 50°C$ for 0 doping of P_2O_5; (iii) $\Delta T = 0°C$ and (iv) $\Delta T = 50°C$ for 1.57 mol. % doping of P_2O_5.

images in the transverse cross-section are observed, and (ii) the focus is much more confined outside the fiber (in air) than within the MMF. The absence of multiple peaks in the transverse cross section can be attributed to the nearly same $\Delta\beta$ among the guided modes of the parabolic index MMF; i.e., the condition of self-imaging is satisfied more rigorously in the parabolic index MMF than in step-index MMF. In Fig. 2(b) we show the effect of temperature on the reimaging/lens action by plotting the intensity distribution outside the MMF for no P_2O_5 [Figs. 2(b)-i and 2(b)-ii] and for 1.57 mol. % P_2O_5 [Figs. 2(b)-iii and 2(b)-iv] at two different temperature differences $\Delta T = 0°C$ and $\Delta T = 50°C$. The axial locations of peak intensity, in Figs. 2(b)-i and 2(b)-ii, are 10320.8 and 10308.3 μm, respectively, giving a large shift of 250 nm /°C in the focal point for P_2O_5 free MMF; the corresponding power difference at the initial focal point is ~19%. These shifts are considerably high considering the MMI's application as a fiber lens for irradiating the biological samples. However, the focal point is temperature independent for the 1.57 mol. % P_2O_5 doped MMF core.

In conclusion, in this Letter we have analyzed the effect of P_2O_5 (in the germanio-silicate MMF core) on the multimodal interference characteristics. We have shown that the intrinsic temperature-independent MMI devices can be obtained employing a MMF core composition of 1.57 mol. % P_2O_5 in 13.5 mol. % GeO_2 doped 84.93 mol. % SiO_2 host for parabolic index core.

References

1. L. B. Soldano and E. C. M. Pennings, J. Lightwave Technol. **13**, 615 (1995).
2. Y. O. Ylmaz, A. Mehta, W. S. Mohammed, and E. G. Johnson, Opt. Lett. **32**, 3170 (2007).
3. W. S. Mohammed, P. W. E. Smith, and X. Gu, Opt. Lett. **31**, 2547 (2006).
4. J. Lopez, A. Guzman, D. Arrioja, R. Aguilar, and P. Wa, Opt. Lett. **35**, 324 (2010).
5. S. M. Tripathi, A. Kumar, E. Marin, and J.-P. Meunier, J. Lightwave Technol. **28**, 3535 (2010).
6. D. M. Mackie and A. W. Lee, Appl. Opt. **43**, 6609 (2004).
7. W. S. Mohammed, A. Mehta, and E. G. Johnson, J. Lightwave Technol. **22**, 469 (2004).
8. E. Li, X. Wang, and C. Zhang, Appl. Phys. Lett. **89**, 091119 (2006).
9. S. M. Tripathi, A. Kumar, E. Marin, and J. P. Meunier, J. Lightwave Technol. **27**, 2348 (2009).
10. S. M. Tripathi, A. Kumar, E. Marin, and J. P. Meunier, IEEE Photon. Technol. Lett. **22**, 799 (2010).
11. E. Li, Opt. Lett. **32**, 2064 (2007).
12. B. Dong, D.-P. Zhou, L. Wei, W.-K. Liu, and J. W. Y. Lit, Opt. Express **16**, 19291 (2008).
13. B. Dong, D.-P. Zhou, L. Wei, W.-K. Liu, and J. W. Y. Lit, J. Lightwave Technol. **28**, 1011 (2010).
14. B. Dong and E. J. Hao, J. Opt. Soc. Am. **28**, 2332 (2011).
15. A. K. Ghatak and K. Thyagarajan, *Introduction to Fiber Optics* (Cambridge Univ., 1998).
16. D. Marcuse, J. Opt. Soc. Am. **68**, 103 (1978).
17. P. Sheng, Phys. Rev. Lett. **45**, 60 (1980).
18. Y. Morishita and K. Tanaka, J. Appl. Phys. **93**, 999 (2003).
19. H. Ticha, J. Schwarz, L. Ticha, and R. Mertens, J. Optoelectron Adv. Mater. **6**, 747 (2004).
20. J. W. Fleming, Electron. Lett. **14**, 326 (1978).
21. J. W. Fleming, J. Am. Ceram. Soc. **59**, 503 (1976).
22. M. J. Adams, *An Introduction to Optical Waveguides* (Wiley, 1981).